JACS
JOURNAL OF THE AMERICAN CHEMICAL SOCIETY

COMMUNICATION

pubs.acs.org/JACS

Electocatalytic Water Oxidation by Cobalt(III) Hangman β-Octafluoro Corroles

Dilek K. Dogutan,[†] Robert McGuire, Jr.,[†] and Daniel G. Nocera*

Department of Chemistry, Massachusetts Institute of Technology, 77 Massachusetts Avenue, Cambridge, Massachusetts 02139-4307, United States

Supporting Information

ABSTRACT: Cobalt hangman corrole, bearing β-octafluoro and *meso*-pentafluorophenyl substituents, is an active water splitting catalyst. When immobilized in Nafion films, the turnover frequencies for the $4e^-/4H^+$ process at the single cobalt center of the hangman platform approach 1 s^{-1}. The pH dependence of the water splitting reaction suggests a proton-coupled electron transfer (PCET) catalytic mechanism.

An attractive approach to meeting the energy demands of a growing global population[1−3] is to capture solar energy and store it in the form of chemical fuels.[4−6] A prevailing solar-to-fuels process is the splitting of water to produce hydrogen,[7] which may be used directly or combined with carbon dioxide to produce a more conventional fuel. The water splitting process is a $4e^-/4H^+$ process, thus providing an imperative for the discovery of new catalysts that bridge the $1e^-/1H^+$ capture process of most light-harvesting systems, including semiconductors, to the $4e^-/4H^+$ process of water splitting. We recently reported that heterogeneous Co-phosphate (Co-Pi)[8−10] and Ni-borate (Ni-Bi)[11] films form self-healing[12] catalysts that promote the efficient splitting of water under benign conditions. XAS studies[13,14] have established that the Co-Pi is a molecular cobaltate catalyst that is a structural relative of the oxygen-evolving complex Photosystem II.[15] With this discovery, we have turned our attention to exploring molecular cobalt catalysts in homogeneous solution because characterization of the catalytic species, the ability to tune catalytic properties, and the mechanism of action is in principle more easily investigated. Several molecular catalysts have been reported recently that demonstrate impressive OER activity.[16−25] A recent report from our laboratory reveals that Co(II) hangman porphyrins promote the $4e^-/4H^+$ reduction of oxygen to water.[26] The oxygen reduction reaction (ORR) is the reverse of the oxygen-evolving reaction (OER). Moreover, the oxygen atoms from two water molecules may be situated within the hangman cleft; one water is in the primary coordination sphere of the metal, whereas another is held in the secondary coordination sphere via hydrogen bonding to the hanging group.[27] These two observations taken together piqued our interest in the possibility that Co hangman corroles may be developed as OER catalysts. Our interest was further bolstered by the report that Mn corroles bearing nitroaromatic *meso* groups[28] and pentadentate Co^{II} complexes[29] are OER catalysts. We now report the synthesis of β-octafluoro hangman corrole (Scheme 1), $CoH^{\beta F}CX\text{-}CO_2H$, and we show that it is the most active OER catalyst among cobalt corroles.

Scheme 1

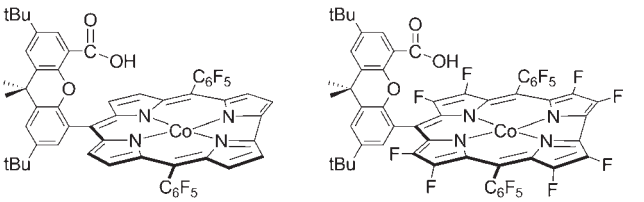

Hangman corroles can be synthesized concisely from easily available starting materials, in two steps, in good yields, and with abbreviated reaction times.[30] In order to boost the oxidizing power of the corrole subunit, we modified the macrocycle with electron-withdrawing groups. Introduction of ancillary fluorinated phenyl groups onto the 5 and 15 *meso*-positions of the framework can increase the oxidizing power of the macrocycle by more than 0.4 V,[31,32] and an additional 0.5−0.6 V[33] is gained upon fluorination of the β-pyrrolic positions of the macrocycle.[34,35] The β-octafluoro hangman corrole was synthesized in 23% overall yield. ^{19}F NMR (Figure S1g) establishes that the *trans*-A_2B isomer is obtained. The relatively high yield in part is due to the use of microwave irradiation, which efficiently drives metal insertion and deprotection of the hanging methyl ester group.[26,30,36] Syntheses and characterization details of new compounds are provided in the Supporting Information.

Samples for electrocatalysis were prepared by dissolving the corrole in a 10:2:1 mixture of THF/ethanol/Nafion solution, to give a final concentration of 0.5% Nafion and 1 mM catalyst. A 30 μL drop of solution was then deposited onto an FTO-coated glass slide and allowed to slowly evaporate. The resulting film contained 30 nmol of catalyst per cm^2.

A cyclic voltammogram (CV) of $CoH^{\beta F}CX\text{-}CO_2H$ in CH_2Cl_2 is shown in Figure S3f. The previously published CVs of $Co(C_6F_5)_3$ and $CoHCX\text{-}CO_2H$ are also reproduced in Figure S3f for convenience.[30] $CoH^{\beta F}CX\text{-}CO_2H$ exhibits a reduction wave at 0.33 V and an oxidation event at 0.87 V vs ferrocene. Addition of water to a DMF solution of the corrole reveals a catalytic peak positive of the reversible oxidation process (Figure S3f) prompting us to examine the electrochemistry in aqueous solutions (0.1 M phosphate buffer, pH = 7). Figure 1 shows that $CoH^{\beta F}CX\text{-}CO_2H$ exhibits

Received: March 8, 2011
Published: May 23, 2011

dx.doi.org/10.1021/ja202138m | J. Am. Chem. Soc. 2011, 133, 9178–9180

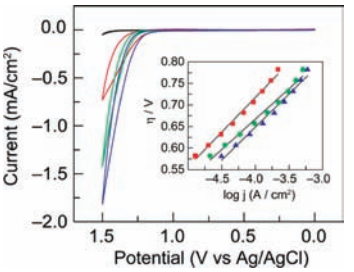

Figure 1. Cyclic voltammograms of FTO background (black) and Nafion films containing 30 nmol/cm^2 of $Co(C_6F_5)_3$ (red, ■), CoHCX-CO_2H (green, ●) and CoH$^{\beta F}$CX-CO_2H (blue, ▲) deposited on FTO glass in 0.1 M KPi buffer, pH 7. Scan rate, 0.1 V/s. Inset: Tafel plots of the same electrodes.

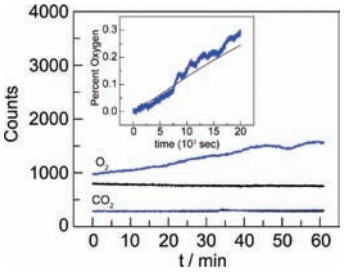

Figure 2. Mass spectrometric detection of O_2 and CO_2 during electrolysis of a bare electrode (−, black) and CoH$^{\beta F}$CX-CO_2H (−, blue) at 1.4 V vs Ag/AgCl. Inset: O_2 production measured by fluorescent sensor (−, blue) and the theoretical amount of O_2 produced (−, black) assuming a Faradaic efficiency of 100%.

greater current and earlier onset of catalytic current as compared to its β-nonfluorinated congener, and both hangman compounds exhibit greater current than the cobalt corrole possessing *meso*-C_6F_5 groups but lacking the hanging group ($Co(C_6F_5)_3$). The onset of the catalytic current (1.25 V vs Ag/AgCl) occurs ∼0.6 V beyond the thermodynamic potential for water oxidation at pH = 7 (0.62 V vs Ag/AgCl); this value is nearly 100 mV higher than that of recently reported molecular cobalt catalysts.[17] The inset in Figure 1 shows the Tafel plots of the three corrole compounds. A slope of ∼120 mV/decade indicates that an electron transfer step is the rate-determining step.[37] The curvature of the Tafel plot indicates a potentially more complex mechanism; however, this curvature is more likely due to the mediation of electron and proton transfer by the Nafion film and not to mechanistic details associated with the intrinsic activity of the catalyst. We note that the "Co^{IV}" hangman corroles are isolable species. We have shown that the spectroscopic properties and DFT calculations of cobalt corrole axially ligated by chloride are consistent with a "Co^{IV}" species that is better described as a Co^{III} site strongly antiferromagnetically coupled to the $S = {}^1/_2$ of the monoradical dianion corrole, [Co^{III}Cl-corrole$^{+\bullet}$].[30] We note that β-fluorination will make the corrole more difficult to oxidize, and therefore, the exact oxidation states of the metal and corrole remain ambiguous. Regardless of the exact nature of the precatalytic state, water oxidation occurs more positive of the first oxidation event of Co^{III}H$^{\beta F}$CX-CO_2H to produce formally Co^{III}H$^{+\bullet\beta F}$CX-CO_2H or Co^{IV}H$^{\beta F}$CX-CO_2H. These results indicate that the active catalytic species is Co^{IV}H$^{+\bullet\beta F}$CX-CO_2H.

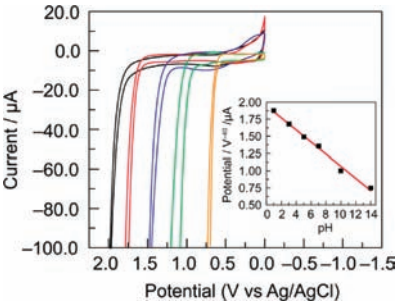

Figure 3. pH dependence of cyclic voltammograms at pH 1, 3, 7, 10, and 14 from left to right. Scan rate is 100 mV/s. Inset: Potential (measured at 40 μA) vs pH with a slope of 88 mV/pH unit.

The Faradaic efficiency of the CoH$^{\beta F}$CX-CO_2H catalyst was measured by using a fluorescence-based O_2 sensor. Electrolysis was performed in aqueous solutions (0.1 M phosphate buffer, pH = 7) in a gastight electrochemical cell under an N_2 atmosphere with the sensor placed in the headspace. After initiating electrolysis at 1.4 V, the percentage of O_2 detected in the headspace rose in accord with what was predicted by assuming that all of the current was caused by 4e$^-$ oxidation of water to produce O_2 (Figure 2 inset). Thus only O_2 is produced during catalytic turnover by CoH$^{\beta F}$CX-CO_2H. The gaseous products evolved during electrolysis at constant potential (1.4 V vs Ag/AgCl, pH = 7) were also measured by mass spectrometry and the results are shown in Figure 2. By this measurement, CoH$^{\beta F}$CX-CO_2H is also observed to be the most efficient catalyst of the series as nearly twice as much oxygen is detected as compared to CoHCX-CO_2H and $Co(C_6F_5)_3$ (Figure S5). Importantly, during the course of the electrolysis, we observe no CO_2, which may result if the corrole framework were to be oxidized. As further testament to catalyst stability, the CoH$^{\beta F}$CX-CO_2H electrode was immersed in THF upon the completion of electrolysis, and the solution was concentrated. UV−vis (Figure S4a), LD-MS MALDI-TOF (Figure S4b), and high-resolution ESI-MS (Figures S4c and S4d) all indicate only the presence of the cobalt hangman corrole. Finally the pH dependence of the OER reaction (Figure 3) shows that the overpotential for OER decreases with increasing pH. A plot of the potential as measured at constant current (40 μA) versus pH shows a monotonic decrease from pH = 14 to pH = 1 (Figure 3, inset). This indicates that decomposition of the catalyst to cobalt oxide is unlikely, as such species are unstable in very acidic solutions. Finally, the onset potentials for the three catalysts are unique and the overpotential for OER is also inconsistent with cobalt oxide-type species.[38]

With OER established, the turnover frequency (TOF) may be calculated by measuring the current density for the 4e$^-$/4H$^+$ OER process of CoH$^{\beta F}$CX-CO_2H. At 1.4 V vs Ag/AgCl, the TOFs per Co atom for CoH$^{\beta F}$CX-CO_2H is 0.81 s^{-1}. This number compares favorably with regard to other cobalt-based water oxidation catalysts.[39,40]

In summary, hangman cobalt corroles are OER catalysts with β-octafluoro Co^{III} xanthene hangman corrole, bearing 5,15-bis-(pentafluorophenyl) substitutients as the most effective OER catalyst. The catalyst is stable under operating conditions and evolves only oxygen as the OER product at modest overpotential. The ability of the hanging group to preorganize water within the hangman cleft appears to be beneficial for the O−O bond-forming reaction of OER.

dx.doi.org/10.1021/ja202138m |*J. Am. Chem. Soc.* 2011, 133, 9178–9180

■ ASSOCIATED CONTENT

Supporting Information. Full synthetic details and characterization for $Co(C_6F_5)_3$, CoHCX-CO_2H, and $CoH^{\beta F}$CX-CO_2H; additional electrochemical data for $Co(C_6F_5)_3$ and $CoH^{\beta F}$CX-CO_2H; and characterization after electrolysis of $CoH^{\beta F}$CX-CO_2H. This material is available free of charge via the Internet at http://pubs.acs.org.

■ AUTHOR INFORMATION

Corresponding Author
nocera@mit.edu

Author Contributions
[†]These authors contributed equally to this work.

■ ACKNOWLEDGMENT

This work was performed under the auspices of the Division of Chemical Sciences, Geosciences, and Biosciences, Office of Basic Energy Sciences of the U.S. Department of Energy through Grant DE-FG02-05ER15745. New synthetic methods were performed under the sole sponsorship of Eni S.p.A under the Eni-MIT Alliance Solar Frontiers.

■ REFERENCES

(1) Lewis, N. S.; Nocera, D. G. *Proc. Natl. Acad. Sci. U.S.A.* **2006**, *103*, 15729.
(2) Abbott, D. *Proc. IEEE* **2010**, *98*, 42.
(3) Nocera, D. G. *Energy Environ. Sci.* **2010**, *3*, 993.
(4) Cook, T. R.; Dogutan, D. K.; Reece, S. Y.; Surendranath, Y.; Teets, T. S.; Nocera, D. G. *Chem. Rev.* **2010**, *110*, 6474.
(5) Gust, D.; Moore, T. A.; Moore, A. L. *Acc. Chem. Res.* **2009**, *42*, 1890.
(6) Nocera, D. G. *Inorg. Chem.* **2009**, *48*, 10001.
(7) Esswein, A. J.; Nocera, D. G. *Chem. Rev.* **2007**, *107*, 4022.
(8) Kanan, M. W.; Nocera, D. G. *Science* **2008**, *321*, 1072.
(9) Surendranath, Y.; Kanan, M. W.; Nocera, D. G. *J. Am. Chem. Soc.* **2010**, *132*, 16501.
(10) Surendranath, Y.; Dincă, M.; Nocera, D. G. *J. Am. Chem. Soc.* **2009**, *131*, 2615.
(11) Dincă, M.; Surendranath, Y.; Nocera, D. G. *Proc. Natl. Acad. Sci. U.S.A.* **2010**, *107*, 10337.
(12) Lutterman, D. A.; Surendranath, Y.; Nocera, D. G. *J. Am. Chem. Soc.* **2009**, *131*, 3838–3839.
(13) Risch, M.; Khare, V.; Zaharieva, I.; Gerencser, L.; Chernev, P.; Dau, H. *J. Am. Chem. Soc.* **2009**, *131*, 6936.
(14) Kanan, M. W.; Yano, J.; Surendranath, Y.; Dincă, M.; Yachandra, V. K.; Nocera, D. G. *J. Am. Chem. Soc.* **2010**, *132*, 13692.
(15) Kanan, M. W.; Surendranath, Y.; Nocera, D. G. *Chem. Soc. Rev.* **2009**, *38*, 109.
(16) Blakemore, J. D.; Schley, N. D.; Balcells, D.; Hull, J. F.; Olack, G. W.; Incarvito, C. D.; Eisenstein, O.; Brudvig, G. W.; Crabtree, R. H. *J. Am. Chem. Soc.* **2010**, *132*, 16017.
(17) Yin, Q.; Tan, J. M.; Besson, C.; Geletti, Y. V.; Musaev, D. G.; Kuznetsov, A. E.; Luo, Z.; Hardcastle, K. I.; Hill, C. L. *Science* **2010**, *328*, 342.
(18) Concepcion, J. J.; Jurss, J. W.; Templeton, J. L.; Meyer, T. J. *J. Am. Chem. Soc.* **2008**, *130*, 16462.
(19) Ellis, W. C.; McDaniel, N. D.; Bernhard, S.; Collins, T. J. *J. Am. Chem. Soc.* **2010**, *132*, 10990.
(20) Mola, J.; Mas-Marza, E.; Sala, X.; Romero, I.; Rodríguez, M.; Viñas, C.; Parella, T.; Llobet, A. *Angew. Chem., Int. Ed.* **2008**, *47*, 5830.
(21) Chen, Z.; Concepcion, J. J.; Jurss, J. W.; Meyer, T. J. *J. Am. Chem. Soc.* **2009**, *131*, 15580.
(22) Sartorel, A.; Miró, P.; Salvaodori, E.; Romain, S.; Carraro, M.; Scorrano, G.; Di Valentin, M.; Llobet, A.; Bo, C.; Bonchio, M. *J. Am. Chem. Soc.* **2009**, *131*, 16051.
(23) Geletii, Y. V.; Besson, C.; Hou, Y.; Yin, Q.; Musaev, D. G.; Quiñonero, D.; Cao, R.; Hardcastle, K. I.; Proust, A.; Kögerler, P.; Hill, C. L. *J. Am. Chem. Soc.* **2009**, *131*, 17360.
(24) McDaniel, N. D.; Coughlin, F. J.; Tinker, L. L.; Bernhard, S. *J. Am. Chem. Soc.* **2008**, *130*, 210.
(25) Hull, J. F.; Balcells, D.; Blakemore, J. D.; Incarvito, C. D.; Eisenstein, O.; Brudvig, G. W.; Crabtree, R. H. *J. Am. Chem. Soc.* **2009**, *131*, 8730.
(26) McGuire, R., Jr.; Dogutan, D. K.; Teets, T. S.; Suntivich, J.; Shao-Horn, Y.; Nocera, D. G. *Chem. Sci.* **2010**, *1*, 411.
(27) Yeh, C.-Y.; Chang, C. J.; Nocera, D. G. *J. Am. Chem. Soc.* **2001**, *123*, 1513.
(28) Gao, Y.; Akermark, T.; Liu, J.; Sun, L.; Akermark, B. *J. Am. Chem. Soc.* **2009**, *131*, 8726.
(29) Wasylenko, D. J.; Ganesamoorthy, C.; Borau-Garcia, J.; Berlinguette, C. P. *Chem. Commun.* **2011**, *47*, 4251.
(30) Dogutan, D. K.; Stoian, S. A.; McGuire, R., Jr.; Schwalbe, M.; Teets, T. S.; Nocera, D. G. *J. Am. Chem. Soc.* **2011**, *133*, 131.
(31) Neya, S.; Funasaki, N. *J. Heterocycl. Chem.* **1997**, *34*, 689.
(32) Woller, E. K.; DiMagno, S. G. *J. Org. Chem.* **1997**, *62*, 1588.
(33) Kadish, K. M.; Caemelbeck, E. V.; Royal, G. In *The Porphyrin Handbook*; Kadish, K. M., Smith, K. M., Guilard, R., Eds.; Academic Press: San Diego, 2000; Vol. 8.
(34) Steene, E.; Dey, A.; Ghosh, A. *J. Am. Chem. Soc.* **2003**, *125*, 16300.
(35) Liu, H.-Y.; Lai, T.-S.; Yeung, L.-L.; Chang, C.-K. *Org. Lett.* **2003**, *5*, 617.
(36) Dogutan, D. K.; Bediako, D. K.; Teets, T. S.; Schwalbe, M.; Nocera, D. G. *Org. Lett.* **2010**, *12*, 1036.
(37) Gileadi, E. *Electrode Kinetics for Chemists, Chemical Engineers, and Materials Scientists*; Wiley-VCH: New York, 1993.
(38) Surendranath, Y.; Nocera, D. G. *Prog. Inorg. Chem.* **2011**, in press.
(39) Esswein, A. S.; Surendranath, Y.; Reece, S. Y.; Nocera, D. G. *Energy Environ. Sci.* **2011**, *4*, 499.
(40) Jiao, F.; Frei, H. *Angew. Chem., Int. Ed.* **2009**, *48*, 1841.